Volume 22, No 4 | International Journal of Radiation Research, October 2024

Value of dynamic contrast-enhanced magnetic resonance imaging quantitative parameters in evaluating the efficacy of neoadjuvant chemoradiotherapy for cervical cancer

M.Yi[1#], R. Hong[2#], Zh. Zhang[3], Z. Xiong[1], J. Ran[1*]

[1]Department of Radiology, Chongqing Fifth People's Hospital, Chongqing, 400062, China
[2]Department of Ultrasound, Affiliated Cancer Hospital of Chongqing University, Chongqing, 400030, China
[3]Department of Radiology, The First Affiliated Hospital of Air Force Military Medical University, Xi'an, 710000, Shaanxi, China

► ***Original article***

***Corresponding author:**
Jing Ran, M.D.,
E-mail:
songxundou32875378@163.com

Received: November 2023
Final revised: February 2024
Accepted: March 2024

Int. J. Radiat. Res., October 2024; 22(4): 1067-1074

DOI: 10.61186/ijrr.22.4.1067

Keywords: *dynamic contrast-enhanced magnetic resonance imaging, quantitative parameters, cervical cancer, neoadjuvant chemotherapy, efficacy evaluation.*

ABSTRACT

Background: this study focused on evaluating the effectiveness of dynamic contrast-enhanced magnetic resonance imaging (DCE-MRI) in patients with cervical cancer (CC) undergoing neoadjuvant chemotherapy and radiation therapy. ***Materials and Methods:*** a total of 58 CC patients were included, undergoing examination through DCE-MRI scans. Subsequently, all cases were divided into two groups: the chemotherapy-effective group (32 cases) including complete response (CR) and partial response (PR), and the chemotherapy-ineffective group (26 cases) including stable disease (SD) and disease progression (PD). ***Results:*** after treatment, the average maximum diameter of tumors in the chemotherapy and radiation therapy failure group was 4.38 ± 1.23 cm, drastically larger than the 2.51±0.64 cm in the chemotherapy and radiation therapy response group ($P < 0.05$). Before treatment, the K^{trans} of the chemotherapy and radiation therapy response group was superior to that of the failure group, while Ve was inferior to the latter ($P < 0.05$). After treatment, the K^{trans} of the chemotherapy and radiation therapy response group decreased, showing a more drastic reduction compared to the failure group ($P < 0.05$). The K^{trans} of the chemotherapy and radiation therapy response group was drastically inferior to that of the failure group, with statistical significance ($P<0.05$). The ΔK^{trans}% in the chemotherapy and radiation therapy response group was negative, inferior to pre-treatment values. In contrast, the ΔK^{trans}% in the chemotherapy and radiation therapy failure group was positive, superior to pre-treatment values ($P < 0.05$). ***Conclusion:*** DCE-MRI demonstrates excellent scanning performance for CC, accurately monitoring the blood flow signals of CC tumors. K^{trans}, Ve, and ΔK^{trans} have high predictive value in neoadjuvant chemotherapy and radiation therapy.

INTRODUCTION

Cervical cancer (CC), as the second leading malignancy among women in China, has seen a rising trend in both incidence and mortality in recent years, posing a significant threat to women's health. Globally, the increasing incidence and mortality cases of CC underscore the urgent need for more effective treatment strategies [1,2]. Particularly for patients with locally advanced CC, traditional treatment approaches face challenges such as low survival rates, high surgical complexity, and susceptibility to recurrence and metastasis. Neoadjuvant chemotherapy (NACT) has garnered widespread attention as a potential therapeutic approach. However, the application of neoadjuvant chemotherapy is not universally applicable, given the variability in patient sensitivity to the treatment [3-5]. Insensitive patients may experience delays in effective treatment time and develop side effects such as cross-resistance due to neoadjuvant chemotherapy. Therefore, accurately identifying patient's sensitive to neoadjuvant chemotherapy is crucial to enhance treatment efficacy [6,7].

Currently, in clinical practice, the evaluation of solid tumor efficacy primarily relies on the response evaluation criteria in solid tumors (RECIST). However, RECIST evaluation exhibits a certain lag in addressing morphological changes such as tumor edema, necrosis, and inflammatory infiltration that may occur after neoadjuvant chemotherapy. This limitation prevents real-time and accurate reflection of changes in tumor burden based on morphological alterations, prompting the urgent need for a novel method of efficacy assessment [8-10]. Against this backdrop, magnetic resonance imaging (MRI) emerges as a tool capable of quantitatively and qualitatively capturing biological processes at the cellular and molecular levels, offering a fresh approach to efficacy assessment. Dynamic contrast-

[DOI: 10.61186/ijrr.22.4.1067]

enhanced MRI (DCE-MRI) combines MRI technology with contrast agents, capturing the dynamic distribution of contrast agents in a continuous sequence of images [11-13]. By observing changes in contrast agents within the image sequence, this technique provides detailed information on tissue perfusion, microcirculation, and vascularization. Patients receive a contrast agent injection before undergoing MRI, typically a drug containing metal ions. This contrast agent enhances the contrast of MRI images. Following the injection of the contrast agent, MRI equipment continuously acquires a series of images, typically involving multiple time points. These images record the distribution and clearance of the contrast agent within the tissue [14-16]. By analyzing the image sequence, dynamic parameters such as the shape of the enhancement curve, maximum intensity, and time to peak can be obtained. These parameters reflect the perfusion and hemodynamic characteristics of the tissue. The application of DCE-MRI in cancer research has been widely recognized, particularly for its significant value in early diagnosis and treatment monitoring of CC [17,18]. DCE-MRI can provide information about tumor vascular perfusion and permeability, aiding in the early detection of CC lesions and enhancing diagnostic accuracy in the early stages. It also assists physicians in accurately locating the extent of CC lesions and provides a detailed description of the biological characteristics of the lesions, facilitating the development of personalized treatment plans. During the treatment of CC, DCE-MRI can be employed to monitor the tumor's response to therapy, assess changes in tumor hemodynamics, and subsequently adjust treatment plans in a timely manner. By analyzing the blood flow parameters of tumor tissues, it can offer prognostic information about CC patients, assisting physicians in better predicting the disease's progression [19-21].

Building upon this, the present study aimed to utilize DCE-MRI to monitor dynamic changes in quantitative parameters within the CC lesion area. In conjunction with RECIST evaluation, it aimed to analyze the characteristic changes in tissues with different proliferation activities and chemotherapy sensitivities. Through an in-depth investigation into early assessment methods for neoadjuvant chemotherapy efficacy in CC, the objective was to provide a theoretical basis for swiftly and effectively determining personalized treatment plans in clinical practice. The innovation of this study lies in the integration of DCE-MRI and RECIST evaluation, allowing not only a focus on morphological changes in tumors but also an emphasis on alterations in local tissue hemodynamics. This comprehensive assessment approach holds the potential to provide comprehensive information for accurately determining chemotherapy sensitivity, and such an integrated evaluation method is anticipated to achieve innovative progress in the field of CC treatment.

MATERIALS AND METHODS

The research participants

A total of 58 CC (CC) patients, ranging in age from 21 to 62 years with an average age of 45.63 ± 8.39 years, were prospectively enrolled from the Department of Gynecology at Chongqing Fifth People's Hospital between August 2022 and August 2023. In accordance with ethical standards, the study received approval from the hospital's ethics committee (Committee Name: Chongqing Fifth People's Hospital, Registration Number: CFPH032, Registration Date: October 4, 2022). Informed consent was obtained from all participants or their authorized representatives.

Patients included in this study met the following criteria: (i) confirmed diagnosis of CC through pathological examination, with gynecological FIGO stage [22] ranging from IB2-IIA to IIB; (ii) no prior antitumor therapy before neoadjuvant treatment; and (iii) absence of contraindications for DCE-MRI.

Exclusion criteria encompassed: (i) patients exhibiting poor compliance and non-cooperation with the examination; (ii) inability to remove the uterine IUD or presence of other metallic foreign bodies that could impact DCE-MRI image quality; and (iii) severe side effects from neoadjuvant therapy leading to premature treatment discontinuation.

Neoadjuvant chemoradiotherapy regimens

Before neoadjuvant chemotherapy was initiated, a meticulous bimanual examination of the patients was conducted. Simultaneously, a detailed inspection of the cervix was performed using a speculum to ensure comprehensive patient understanding and accurate assessment. The core drug selected for the neoadjuvant chemotherapy regimen was cisplatin (TP regimen), and the specific procedural steps of the regimen are outlined as follows:

(1) Drug dosage: the equation by Stevenson was employed for body surface area calculation [23] to calculate the dosage of paclitaxel and cisplatin based on individual patient characteristics, ensuring a personalized and precise approach throughout the treatment process. Equation (1) was for body surface area calculation, equation (2) was for paclitaxel total dose calculation, and equation (3) was for cisplatin total dose calculation.

(2) Paclitaxel administration: the total dose of paclitaxel was administered on the first day of treatment, delivered slowly and continuously over 3 hours using an infusion pump. This infusion method aimed to maximize the therapeutic effects of the drug while minimizing patient discomfort.

(3) Cisplatin administration: the total dose of

[DOI: 10.61186/ijrr.22.4.1067]

cisplatin was divided into three parts, with treatment commencing on the first day. These three portions of the drug were administered over three days through intravenous infusion. This fractionated drug administration strategy not only helps mitigate the burden on the body but also aids in better controlling adverse reactions during the course of treatment.

The use of the TP regimen with cisplatin as the main drug took into consideration individual variations. By employing a fractionated drug administration approach, the regimen aimed to maximize efficacy, minimize adverse reactions, and ensure treatment precision and personalization through detailed patient observation before treatment initiation.

Body surface area (m^2) = 0.0061 × height (cm) + 0.0128 × weight (kg) - 0.1529 (1)

Total taxol (mg) = 175mg / m^2 × Body surface area (m^2) (2)

Total cisplatin(mg) = 75mg / m^2 ×Body surface area (m^2) (3)

DCE-MRI scan

Four examinations were scheduled during neoadjuvant chemoradiotherapy: before neoadjuvant chemoradiotherapy (MRI $_{pre}$), 2 weeks after treatment (MRI $_{2nd}$), 4 weeks after treatment (MRI $_{4th}$), and 1 month after the end of treatment (MRI $_{post}$). Each examination consisted of a conventional plain scan and DCE-MRI.

All MRI scans in this study were performed on the same 3.0T MRI scanner (Philips, the Netherlands) with patients in the supine position, head first, and breathing freely. The scanning was executed from the upper edge of the wing to the lower edge of the pubic symphysis, covering the entire pelvic cavity. The coil was a 16-channel Torsopa phased array body coil matched with the machine.

Conventional plain scan sequence included T1 cross-sectional (TR 658ms/TE 10.0ms, FOV 240 × 200 mm, layer thickness 5.5 mm, and matrix 256 × 246), T2 sagittal plane (TR 3,000ms, TE 104ms, FOV 240 × 200 mm, layer thickness 3 mm, and matrix 320 × 275) and T2 high-resolution cross-sectional sequence (TR 4,000ms/TE 100ms, FOV 200 × 180 mm, layer thickness 3 mm, and matrix 320 × 320).

DCE-MRI scans were conducted using time-resolved random orbit imaging technology to perform fast multiphase dynamic enhancement scanning sequences of volume interpolated body parts. The main parameters were 2°, 15°, TR of 4.43 ms, TE of 1.50 ms, FOV of 260 mm, 3.6 mm of layer thickness, and 138 × 192 of matrix. Gadolinium diamine injection was used as a contrast agent for enhanced scanning, and 0.2 mL/kg was injected intravenically with 2.5 mL/s by a high-pressure syringe. After injection of contrast agent, 15 mL normal saline was used to flush the tube. The contrast agent was injected before (8 s, 14 s, 20 s, 26 s, 32 s) and after (33 s) injection. A total of 70 scans were performed, and the single scanning time was 4 s. The dynamic enhancement scanning time was 32 s.

Image postprocessing and data measurement

Data were processed by the Siemens Sygno workstation software package (Siemens AG, Germany) and GE OmniKinetics workstation software package (General Electric, USA). The Extended Tofts two-compartment model was utilized for computation. Generation-related parameters included the volume transfer constant (K^{trans}), fractional EES volume (V_e) of the extracellular extravascular space, rate constant (K_{ep}), and fractional plasma volume (V_p) of the contrast agent, which were tested repeatedly three times and averaged. Figure 1 shows the details. Equations (4-7) represent the calculation equations for the average changes in K^{trans}, V_e, K_{ep}, and V_p. Equations (8-11) represent the calculation equations for the average percentage changes in K^{trans}, V_e, K_{ep}, and V_p.

Change value of K^{trans} (ΔK^{trans}) = K^{trans} after NACT treatment-K^{trans} before NACT treatment (4)

Change value of K_{ep} (ΔK_{ep}) = K_{ep} after NACT treatment -K_{ep}before NACT treatment (5)

Change value of V_e (ΔV_e) = V_e after NACT treatment-V_e before NACT treatment (6)

Change value of V^p (ΔV^p) = V^p after NACT treatment-V^p before NACT treatment (7)

$$K^{trans}\ change\ rate\left(\Delta K^{trans}\%\right) = \frac{K^{trans}\ after\ NACT\ treatment - K^{trans}\ before\ NACT\ treatment}{K^{trans}\ before\ NACT\ treatment} \quad (8)$$

$$K_{ep}\ change\ rate\left(\Delta K_{ep}\%\right) = \frac{K_{ep}\ after\ NACT\ treatment - K_{ep}\ before\ NACT\ treatment}{K_{ep}\ before\ NACT\ treatment} \quad (9)$$

$$V_e change\ rate\left(\Delta V_e\%\right) = \frac{V_e after\ NACT\ treatment - V_e before\ NACT\ treatment}{V_e before\ NACT\ treatment} \quad (10)$$

$$V_p change\ rate\left(\Delta V_p\%\right) = \frac{V_p after\ NACT\ treatment - V_p before\ NACT\ treatment}{V_p before\ NACT\ treatment} \quad (11)$$

Measurement of quantitative parameters of DCE-MRI

The DCE-MRI images were processed using GE *OmniKinetics*. Before and after neoadjuvant chemoradiotherapy, two independent radiologists identified the boundaries of the largest tumor layer

[DOI: 10.61186/ijrr.22.4.1067]

based on high-resolution T2WI images. Subsequently, a surgeon manually outlined the region of interest (ROI) at the largest tumor level, as well as the adjacent upper and lower levels on the contrast-enhanced images. To ensure accuracy, the ROI was irregularly delineated in accordance with tumor morphology, aiming to avoid areas of liquefaction, necrosis, and hemorrhage (figure 2). In cases where the residual tumor boundary could not be conclusively determined post-treatment, the ROI was positioned on the MRI image acquired prior to neoadjuvant chemoradiotherapy, corresponding to the tumor ROI.

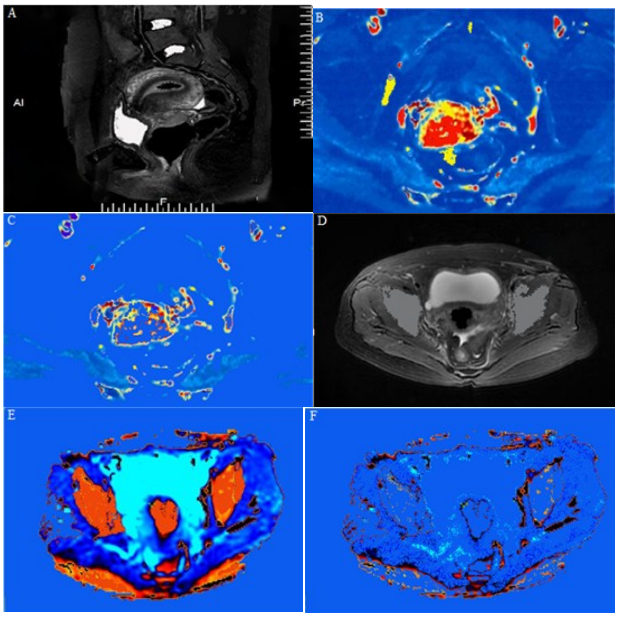

Figure 1. Pseudocolor images of Ktrans, Kep, Vp, and Ve on DCE-MRI. **A:** Sagittal view **B:** Ktrans pseudocolor image (the tumor area was dominated by large patches of red); **C:** Ve pseudocolor map (the tumor area was dominated by a large blue area); **D:** transverse view **E:** Kep pseudocolor map (the tumor area was dominated by a large red area); **F:** Vp pseudocolor map (the tumor area was dominated by a large blue area).

DCE-MRI arterial input function

The DCE-MRI images were transferred to GE *OmniKinetics* for processing. The external iliac artery was selected as the input artery, and its time signal-intensity curve, namely, arterial input function (AIF), was measured (figure 3).

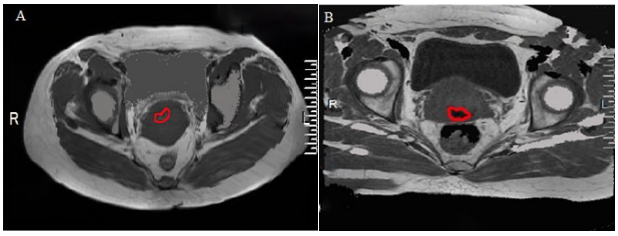

Figure 2. Delineation of the ROI on DCE-MRI images of CC. **A:** stage I; **B:** stage IIA.

DCE-MRI arterial input function

The DCE-MRI images were transferred to GE OmniKinetics for processing. The external iliac artery was selected as the input artery, and its time signal-intensity curve, namely, arterial input function (AIF), was measured (figure 3).

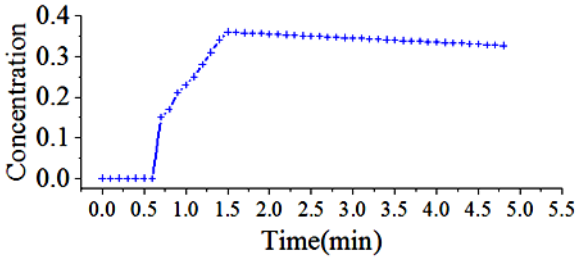

Figure 3. Time signal-intensity curve.

Efficacy evaluation indexes

Tumor response was assessed by two radiologists in a double-blind manner, combining sequences before and after neoadjuvant chemoradiotherapy. Tumor response was classified according to RECIST criteria. Complete response (CR) refers to complete disappearance of all lesions. Partial response (PR) means a reduced value in the maximal diameter of the baseline lesion of ≥ 30%. Progression (PD) refers to an increase in the maximal diameter of the baseline lesion of ≥ 20%. Stable disease (SD) represents the change in maximum diameter between PR and PD. Then, all cases were rolled into two groups, namely, the chemoradiotherapy response group, encompassing CR and PR, and the chemoradiotherapy failure group, including SD and PD.

Statistical analysis

Employing SPSS 20.0 (SPSS, USA), measurement data were represented as ($\bar{x} \pm s$), and were tested by paired data t test; otherwise, the Mann–Whitney test was adopted. Count data were denoted as percentages/frequencies, and the χ^2 test was employed. The longest diameter, quantitative parameters, change value, and change rate of the tumor before and after neoadjuvant chemoradiotherapy were subjected to tests for normal distribution and homogeneity of variance. $P<0.05$ indicated a statistical significance.

RESULTS

Clinical data statistics

A total of 58 patients with CC were enrolled, as mentioned in above section. According to RECIST evaluation criteria, they were grouped into a chemoradiotherapy response group (32/58) and a chemoradiotherapy failure group (26/58). The clinical data of the two groups before treatment were statistically analyzed (table 1).

Changes in the longest diameter of the tumor before and after treatment

In figure 4, before treatment, there was neglectable difference in the mean tumor longest

[DOI: 10.61186/ijrr.22.4.1067]

diameter between the effective treatment group and the ineffective treatment group (P > 0.05), indicating comparable tumor sizes in both groups before treatment. However, after treatment, the mean tumor longest diameter in the ineffective treatment group greatly increased to (4.38 ± 1.23) cm, while in the effective treatment group, it was (2.51 ± 0.64) cm, demonstrating a marked difference between the two groups (P < 0.05). This indicates that post-treatment, the tumors in the effective treatment group drastically reduced in size, while those in the ineffective treatment group exhibited a trend of growth.

Table 1. Clinical data statistics before treatment.

Index	Chemoradio-therapy response group (n=32)	Chemoradio-therapy failure group (n=26)	*P*
Age (years old)	43.36 ± 9.24	45.67 ± 8.18	0.241
Clinical staging [n (%)]			0.163
IB2	7 (21.87)	6 (23.07)	
IIA	2 (6.25)	1 (3.84)	
IIB	23 (71.87)	19 (73.07)	
Pathological Classification [n (%)]			0.287
Squamous cell carcinoma	25 (78.12)	21 (80.76)	
Adenocarcinoma	4 (12.5)	3 (11.53)	
Adenosquamous carcinoma	3 (9.37)	2 (7.69)	
Maximum tumor diameter (cm)	5.73 ± 1.82	5.46 ± 1.74	0.121

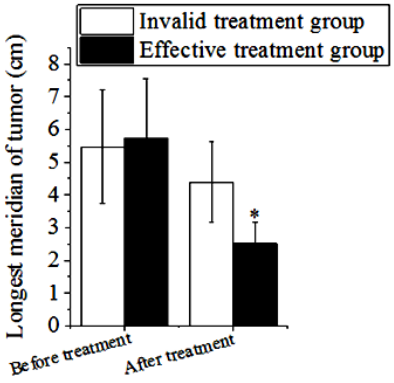

Figure 4. Changes in the longest tumor diameter before and after neoadjuvant therapy. *Note: *P < 0.05 vs. chemoradiotherapy failure group.*

Changes in DCE-MRI quantitative parameters

In figure 5, before treatment, the K^{trans} values in the effective treatment group were superior to those in the ineffective treatment group, while the V_e values were markedly inferior to those in the ineffective treatment group (P < 0.05). After treatment, the K^{trans} levels in the effective treatment group drastically decreased versus the ineffective treatment group (P < 0.05). In contrast, the K_{ep}, V_e and V_p values differed slightly between the two groups before and after treatment (P > 0.05). This indicates that post-treatment, there were drastic changes in tumor hemodynamics in the effective treatment group, while the changes in other parameters were neglectable.

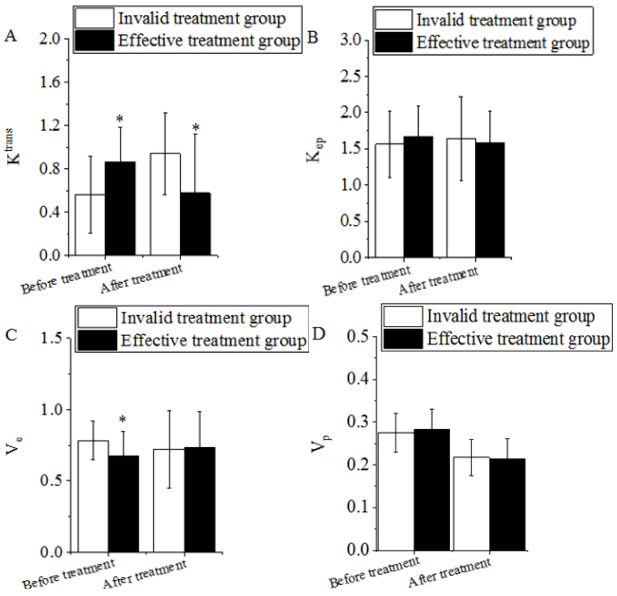

Figure 5. Changes in DCE-MRI quantitative parameters. **A:** Ktrans; **B:** Kep; **C:** Ve; **D:** Vp. *Note: *P < 0.05 vs. chemoradiotherapy failure group.*

Comparison on change value and change rate of DCE-MRI quantitative parameters

In figure 6, post-treatment, the ΔK^{trans} values in the effective treatment group were drastically inferior to those in the ineffective treatment group (P < 0.05). In contrast, the changes in ΔK_{ep}, ΔV_e, and ΔV_p showed neglectable differences between groups (P > 0.05). This suggests that the post-treatment changes in tumor hemodynamics were more pronounced in the effective treatment group, while changes in other parameters are relatively subdued.

In figure 7, post-treatment, the ΔK^{trans}% in the effective treatment group was negative, showing a decrease versus pre-treatment; in contrast, the ineffective treatment group exhibited a positive ΔK^{trans}%, indicating an increase versus pre-treatment. The two groups demonstrated marked difference (P < 0.05). Conversely, changes in ΔK_{ep}%, ΔV_e%, and ΔV_p% showed inconsiderable differences between groups (P > 0.05). This suggests that the post-treatment changes in tumor hemodynamics in the effective treatment group exhibited a negative trend, while the ineffective treatment group showed a positive trend, with remarkable difference between the two.

DCE MRI images

Case 1 was a 45-year-old female. The patient was pathologically confirmed to have stage IIB cervical squamous cell carcinoma by transvaginal biopsy. According to RECIST criteria, this patient was PR and belonged to the chemoradiotherapy response group. The tumor diameter was approximately 5.4 cm before neoadjuvant therapy and 2.3 cm after 1 month of treatment. Before chemoradiotherapy, K^{trans}=0.378

[DOI: 10.61186/ijrr.22.4.1067]

min^{-1}, K_{ep}= 2.198 min^{-1}, V_e=0.362 min^{-1}, and V_p=0.326 min^{-1}. One month after treatment, K^{trans}=0.271 min^{-1}, K_{ep}= 1.621 min^{-1}, V_e=0.815 min^{-1}, and V_p=0.134 min^{-1} (figure 8).

Case 2 was a 53-year-old female. The patient was pathologically confirmed to have stage IA2 cervical squamous cell carcinoma by vaginal biopsy. According to RECIST criteria, the patient was SD and belonged to the chemoradiotherapy response group. The tumor diameter was approximately 6.3 cm before neoadjuvant therapy and 1.9 cm after 1 month of treatment. Before chemoradiotherapy, K^{trans} = 0.563 min^{-1}, K_{ep}= 1.624 min^{-1}, V_e = 0.462 min^{-1}, and V_p = 0.754 min^{-1}. One month after treatment, K^{trans} = 0.657 min^{-1}, K_{ep} = 1.643 min^{-1}, V_e = 0.328 min^{-1}, and V_p = 0.746 min^{-1} (figure 9).

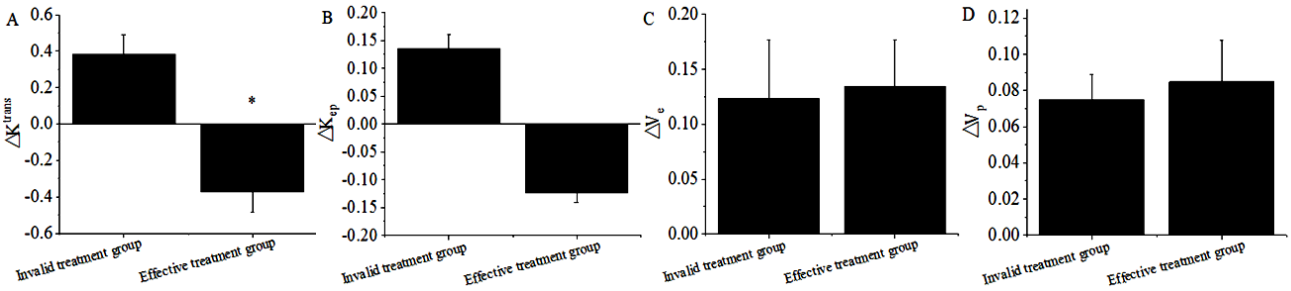

Figure 6. Comparison of DCE-MRI quantitative parameters. **A:** ΔKtrans; **B:** ΔKep; **C:** ΔVe; **D:** ΔVp.
*Note: *P<0.05 vs. chemoradiotherapy failure group.*

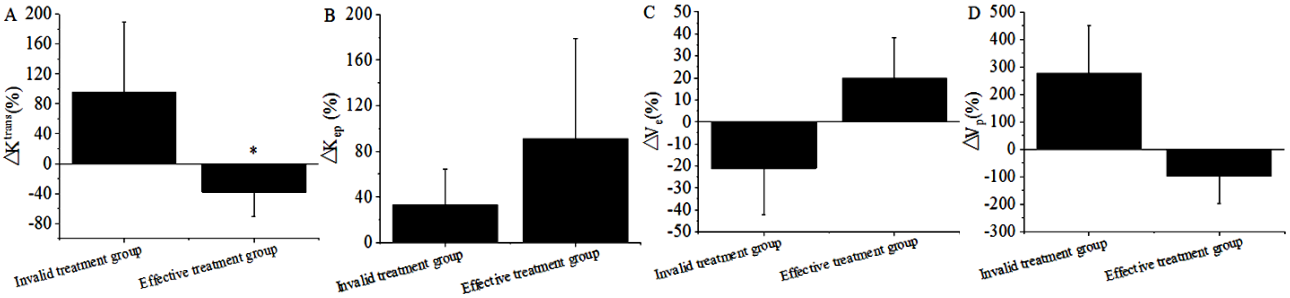

Figure 7. Comparison of the change rate of DCE-MRI quantitative parameters. **A:** ΔKtrans (%); **B:** ΔKep (%); **C:** ΔVe (%); **D:** ΔVp (%).
*Note: *P < 0.05 vs. chemoradiotherapy failure group.*

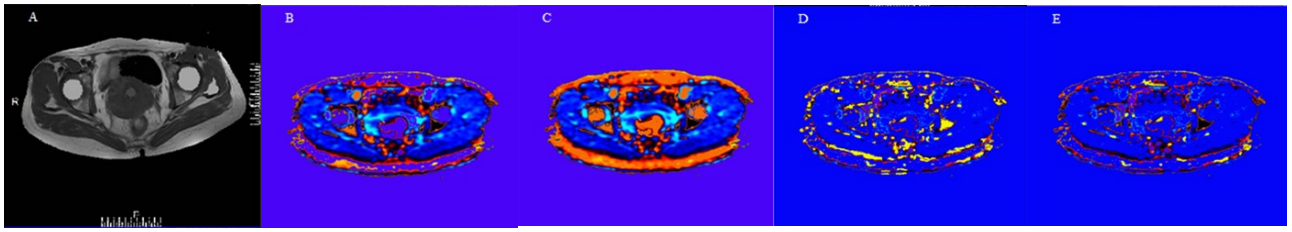

Figure 8. Case 1 DCE-MRI images. (The patient was a 45-year-old female.) **A:** cross-sectional T2WI; **B:** Ktrans; **C:** Kep; **D:** Ve; **E:** Vp.

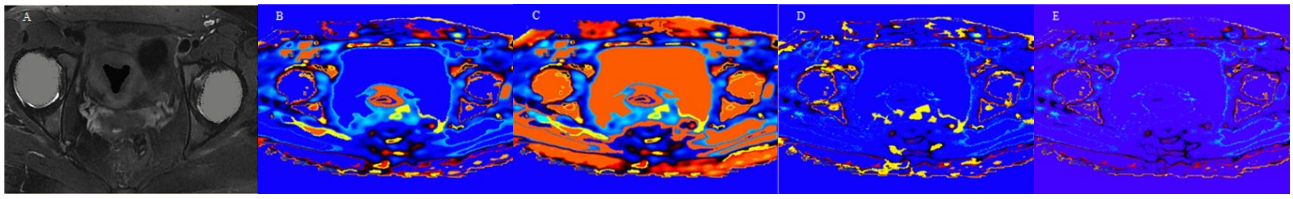

Figure 9. Case 2 DCE-MRI images. (The patient was a 53-year-old female.) **A:** cross-sectional T2WI; **B:** Ktrans; **C:** Kep; **D:** Ve; **E:** Vp.

DISSCUSION

In the treatment of locally advanced CC, neoadjuvant chemotherapy has played a significant role in reducing tumor volume and improving the rate of negative surgical margins [24]. This study employed DCE-MRI to quantitatively observe the parameters in CC patients before and after neoadjuvant treatment, with a particular focus on discussing the pivotal roles of K^{trans}, V_e and ΔK^{trans} in efficacy assessment, as well as their potential clinical value. K^{trans}, serving as an indicator of vascular permeability, plays a crucial role in the changes before and after treatment. The results of this study demonstrated that the K^{trans} level in the effective treatment group was superior to that in the ineffective treatment group before therapy, while the K^{trans} level drastically decreased in the effective treatment group after therapy. This suggests that K^{trans} exhibits sensitivity in evaluating the efficacy of neoadjuvant chemotherapy in CC, with its changes reflecting significant alterations in tumor vascular

[DOI: 10.61186/ijrr.22.4.1067]

perfusion and permeability. In patients responding well to treatment, the decrease in K^{trans} may indicate a reduction in vascular permeability, creating favorable conditions for the shrinkage of the tumor region. Conversely, the limited decrease in K^{trans} levels in the ineffective treatment group suggests the presence of more fibrous tissue, poor tissue permeability and consequently, poorer chemotherapy outcomes. This underscores the importance of K^{trans} in the assessment of treatment efficacy in CC, positioning it as a critical parameter for guiding treatment strategies.

V_e, as a parameter measuring the extracellular extravascular space, indicates that smaller values suggest a smaller extracellular space, facilitating the entry of chemotherapeutic agents into tumor cells. In this study, the pre-treatment effective treatment group exhibited lower V_e values compared to the ineffective treatment group, potentially creating favorable conditions for the tumor shrinkage or disappearance observed in the effective treatment group after therapy. The reduced difference in V_e values between the two groups post-treatment may be associated with the shrinkage of the tumor region in the effective treatment group and local changes in tissue structure. Therefore, V_e holds significant value in predicting outcomes before neoadjuvant treatment, providing clinicians with more precise treatment plan options. The changes in ΔK^{trans} in this study manifested as negative values in the effective treatment group and positive values in the ineffective treatment group. ΔK^{trans} can reflect changes in DCE-MRI image parameters, where smaller values indicate a smaller degree of K^{trans} change, typically associated with poorer treatment outcomes. Conversely, when treatment outcomes are favorable, K^{trans} drastically decreases. This emphasizes the potential role of ΔK^{trans} in the prognostic assessment of neoadjuvant treatment for CC, offering clinicians an intuitive and actionable indicator.

Bhardwaj *et al*. (2022) conducted an experiment aiming to assess the additional value of DWI and DCE -MRI in the preoperative evaluation of CC [25]. The study employed a prospective design, including 45 histologically confirmed CC patients, assessed through local cavity examination and pelvic MRI. Their experimental results demonstrated differences in the mean ADC values among CC patients at different stages. Through ROC curve analysis, they found that the percentage change in arterial-phase signal intensity on DCE-MRI exhibited high sensitivity and specificity in distinguishing stage I CC. Additionally, ADC values showed variations across different stages of CC. In comparison with their experimental findings, our study similarly underscores the importance of DCE-MRI in the assessment of CC. Both studies indicated the value of DCE-MRI in the assessment of CC. While Bhardwaj et al.'s experiment primarily focused on early diagnosis and preoperative staging of CC, our study emphasized monitoring the effectiveness of neoadjuvant chemotherapy. Bhardwaj *et al*.'s research aimed at providing insights into the early detection and preoperative staging of CC, whereas our study focused on supplying information for personalized adjustments during the treatment process. In summary, both studies underscore the crucial role of DCE-MRI in CC research, providing clinicians with rich information for formulating more precise treatment plans. Quantitative parameters of DCE-MRI exhibit significant clinical value in the evaluation of neoadjuvant chemotherapy efficacy for CC. Changes in K^{trans}, V_e and ΔK^{trans} can sensitively reflect alterations in hemodynamics and microcirculation before and after treatment, offering comprehensive information to clinicians for devising more individualized treatment strategies.

Despite some limitations, such as a relatively small sample size and the absence of tumor volume measurements, this study provides robust support for neoadjuvant treatment in CC, offering valuable insights for future clinical practices. Further research efforts should be directed towards enlarging the sample size, delving deeper into the correlation between DCE-MRI parameters and the efficacy of neoadjuvant chemotherapy in CC, and conducting comprehensive evaluations by incorporating additional clinical indicators. Moreover, with the continuous advancement of medical imaging technologies, the introduction of other advanced imaging methods could be considered to enhance our understanding of tumor biological characteristics. In clinical practice, timely and accurate assessment of CC patients' response to neoadjuvant chemotherapy is crucial for devising personalized treatment plans. DCE-MRI, as a non-invasive imaging technique, with its highly sensitive quantitative parameters, provides clinicians with a means to monitor dynamic changes in tumors throughout the treatment cycle. Through detailed analysis of indicators such as K^{trans}, V_e, ΔK^{trans}, physicians can gain a more comprehensive understanding of the patient's condition and make timely adjustments during treatment, thus elevating the level of individualized care.

CONCLUSION

DCE-MRI demonstrated excellent scanning efficacy in capturing CC masses' blood flow signals accurately. The parameters K^{trans}, V_e, and ΔK^{trans} exhibited significant prognostic value in the context of neoadjuvant chemoradiotherapy for CC. Nevertheless, limitations in this study are acknowledged, including a relatively small sample size and constrained efficacy evaluation methods. Further exploration in subsequent stages is warranted to construct a comprehensive evaluation

[DOI: 10.61186/ijrr.22.4.1067]

mechanism. This study, consequently, contributes to establishing a theoretical foundation for promptly and effectively determining personalized and efficient treatment plans for CC patients.

ACKNOWLEDGMENT

We express our gratitude to all individuals and institutions who contributed to the completion of this research. Special thanks are extended to the patients who voluntarily participated in the study and the healthcare professionals who provided support during the process of data collection and experimentation.

Funding Support: This research was funded by [Grant/Award Number], provided by [Funding Agency]. The financial support from these funds played a crucial role in facilitating the data collection, analysis, and interpretation, contributing drastically to the overall success of the study.

Conflict of Interest: The authors of this study declare no financial interests or conflicts that could potentially influence the results and interpretation of the research.

Ethical Considerations: The research protocol received approval from the [Committee Name: Chongqing Fifth People's Hospital, Registration Number: CFPH032, Registration Date: October 4, 2022], and ethical principles outlined in the Helsinki Declaration were adhered to throughout the entire study. Informed consent was obtained from all participants before the commencement of the study to ensure their rights and privacy were adequately protected.

***Author Contributions*:** M.Y., was responsible for research design, data collection, and analysis, and the primary contributor to paper writing. R.H., was involved in data collection and analysis, providing significant support to the writing of the paper. Z.Z., provided valuable suggestions in research design and experimental processes, participated in data interpretation, and contributed to paper revisions. Z.X., was responsible for experiment execution and data organization, offering crucial insights into result interpretation. J.R., was involved in research design and literature review, making important contributions to the structure and content of the paper. The combined contributions of these authors played a pivotal role in the successful completion of the entire research.

REFERENCES

1. Hu Z and Ma D (2018) The precision prevention and therapy of HPV -related cervical cancer: new concepts and clinical implications. *Cancer Med,* ***7(10):*** *5217-5236.*
2. Anil V, Turukmane A, Nawaf Alhebaishi B, Abdulrhman M, Alshareef (2022) Multispectral image analysis for monitoring by IoT based wireless communication using secure locations protocol and classification by deep learning techniques. *Optik,* ***271:*** *170122.*
3. Saleh M, Virarkar M, Javadi S, Elsherif SB, de Castro Faria S, Bhosale P (2020) Cervical Cancer: 2018 Revised International Federation of Gynecology and Obstetrics Staging System and the Role of Imaging. *AJR Am J Roentgenol,* ***214(5):*** *1182-1195.*
4. Gadducci A and Cosio S (2020) Neoadjuvant Chemotherapy in Locally Advanced Cervical Cancer: Review of the Literature and Perspectives of Clinical Research. *Anticancer Res,* ***40(9):*** *4819-4828.*
5. Anupong Wongchai A, Durga rao Jenjeti BA, Indira P (2022) Farm monitoring and disease prediction by classification based on deep learning architectures in sustainable agriculture. *Ecological Modelling,* ***474:*** *110167.*
6. Arvind K, Nishant S, Arpit B (2022) Clinical risk assessment of chronic kidney disease patients using genetic programming. *Computer Methods in Biomechanics and Biomedical Engineering,* ***25(8):*** *887-895.*
7. Benson R, Pathy S, Kumar L, Mathur S, Dadhwal V, Mohanti BK (2019) Locally advanced cervical cancer - neoadjuvant chemotherapy followed by concurrent chemoradiation and targeted therapy as maintenance: A phase II study. *J Cancer Res Ther,* ***15(6):*** *1359-1364.*
8. Noll F, Palacios Torres AT, Pecci P, Lucchini SM, Heredia F (2021) Neoadjuvant chemotherapy in early-stage cervical cancer (< 2 cm) before conization for fertility preservation: is there any advantage over upfront conization? *Int J Gynecol Cancer,* ***31(3):*** *379-386.*
9. Harshit B, Pradeep T, Aditi S (2021) EEG-Based Personality Prediction Using Fast FourierTransfoim and DeepLSTM Model. *Comput Intell Neurosci,* ***2021:*** *6524858.*
10. Lu H, Wu Y, Liu X, Huang H, Jiang H, Zhu C, Man Y, Liu P, Li X, Chen Z, Long X, Pang Q, Deng S, Gu J (2021) The Role of Dynamic Contrast-Enhanced Magnetic Resonance Imaging in Predicting Treatment Response for Cervical Cancer Treated with Concurrent Chemoradiotherapy. *Cancer Manag Res,* ***13:*** *6065-6078.*
11. Zhang A, Song J, Ma Z, Chen T (2020) Combined dynamic contrast-enhanced magnetic resonance imaging and diffusion-weighted imaging to predict neoadjuvant chemotherapy effect in FIGO stage IB2-IIA2 cervical cancers. *Radiol Med,* ***125(12):*** *1233-1242.*
12. Li XX, Lin TT, Liu B, Wei W (2020) Diagnosis of Cervical Cancer with Parametrial Invasion on Whole-Tumor Dynamic Contrast-Enhanced Magnetic Resonance Imaging Combined with Whole-Lesion Texture Analysis Based on T2- Weighted Images. *Front Bioeng Biotechnol,* ***8:*** *590.*
13. Zhang Z, Wang Z, Zhao R (2018) Dynamic Contrast-Enhanced Magnetic Resonance Imaging of Advanced Cervical Carcinoma: The Advantage of Perfusion Parameters from the Peripheral Region in Predicting the Early Response to Radiotherapy. *Int J Gynecol Cancer,* ***28(7):*** *1342-1349.*
14. Treutlein C, Stollberg A, Scherl C, Agaimy A, Ellmann S, Iro H, Lell M, Uder M, Bäuerle T (2020) Diagnostic value of 3D dynamic contrast-enhanced magnetic resonance imaging in lymph node metastases of head and neck tumors: a correlation study with histology. *Acta Radiol Open,* ***9(8):*** *2058460120951966.*
15. Qin F, Pang H, Ma J, Zhao M, Jiang X, Tong R, Yu T, Luo Y, Dong Y (2021) Combined dynamic contrast enhanced MRI parameter with clinical factors predict the survival of concurrent chemoradiotherapy in patients with 2018 FIGO IIICr stage cervical cancer. *Eur J Radiol,* ***141:*** *109787.*
16. Bi Q, Chen Y, Chen J, Zhang H, Lei Y, Yang J, Zhang Y, Bi G (2021) Predictive value of T2-weighted imaging and dynamic contrast-enhanced MRI for assessing cervical invasion in patients with endometrial cancer: a meta-analysis. *Clin Imaging,* ***78:*** *206-213.*
17. Shao J, Zhang Z, Liu H, Song Y, Yan Z, Wang X, Hou Z (2020) DCE-MRI pharmacokinetic parameter maps for cervical carcinoma prediction. *Comput Biol Med,* ***118:*** *103634.*
18. Lund KV, Simonsen TG, Kristensen GB, Rofstad EK (2019) Pharmacokinetic analysis of DCE-MRI data of locally advanced cervical carcinoma with the Brix model. *Acta Oncol,* ***58(6):*** *828-837.*
19. Liu B, Sun Z, Ma WL, Ren J, Zhang GW, Wei MQ, Hou WH, Hou BX, Wei LC, Huan Y, Zheng MW (2020) DCE-MRI Quantitative Parameters as Predictors of Treatment Response in Patients with Locally Advanced Cervical Squamous Cell Carcinoma Underwent CCRT. *Front Oncol,* ***10:*** *585738.*
20. Hauge A, Gaustad JV, Huang R, Simonsen TG, Wegner CS, Andersen LMK, Rofstad EK (2019) DCE-MRI and Quantitative Histology Reveal Enhanced Vessel Maturation but Impaired Perfusion and Increased Hypoxia in Bevacizumab-Treated Cervical Carcinoma. *Int J Radiat Oncol Biol Phys,* ***104(3):*** *666-676.*
21. Lu Y, Peng W, Song J, Chen T, Wang X, Hou Z, Yan Z, Koh TS (2019) On the potential use of dynamic contrast-enhanced (DCE) MRI parameters as radiomic features of cervical cancer. *Med Phys,* ***46 (11):*** *5098-5109.*
22. Merz J, Bossart M, Bamberg F, Eisenblaetter M (2020) Revised FIGO Staging for Cervical Cancer - A New Role for MRI. *Rofo,* ***192 (10):*** *937-944. English, German.*
23. Girens R, Bukoski A, Maitz CA, Boston SE, Borgatti A, Sprinkle M, Orrego D, Kesl S, Selting K (2019) Use of computed tomography and radiation therapy planning software to develop a novel formula for body surface area calculation in dogs. *J Vet Intern Med,* ***33(2):*** *792-799.*
24. Li X, Wu S, Li D, Yu T, Zhu H, Song Y, Meng L, Fan H, Xie L (2019) Intravoxel Incoherent Motion Combined with Dynamic Contrast-Enhanced Perfusion MRI of Early Cervical Carcinoma: Correlations Between Multimodal Parameters and HIF-1α Expression. *J Magn Reson Imaging,* ***50(3):*** *918-929.*
25. Bhardwaj R, Boruah DK, Gogoi BB, Zahir F, Sharma A (2022) Added-Value of Diffusion-Weighted Imaging (DWI) and Dynamic Contrast-Enhanced (DCE-MRI) Magnetic Resonance Imaging in the Preoperative Assessment of Cervical Cancer. *J Obstet Gynaecol India,* ***72(4):*** *330-340.*

[DOI: 10.61186/ijrr.22.4.1067]